

1           **Title: SARS-CoV-2 subgenomic RNA kinetics in longitudinal clinical samples**

2

3   **Authors:**

4   Renu Verma<sup>1</sup>, Eugene Kim<sup>1</sup>, Giovanni Joel Martinez-Colón<sup>1</sup>, Prasanna Jagannathan<sup>1</sup>, Arjun  
5   Rustagi<sup>1</sup>, Julie Parsonnet<sup>1,2</sup>, Hector Bonilla,<sup>1</sup> Chaitan Khosla<sup>3</sup>, Marisa Holubar,<sup>1</sup> Aruna  
6   Subramanian,<sup>1</sup> Upinder Singh<sup>1</sup>, Yvonne Maldonado<sup>4</sup>, Catherine A. Blish,<sup>1</sup> Jason R. Andrews<sup>1</sup>

7       1. Division of Infectious Diseases and Geographic Medicine, Stanford University School of  
8       Medicine, Stanford, CA, USA

9       2. Department of Epidemiology and Population Health Stanford University School of  
10      Medicine, Stanford, CA, USA

11      3. Departments of Chemistry and Chemical Engineering, Stanford University, Stanford,  
12      California 94305, United States

13      4. Department of Pediatrics, Stanford University School of Medicine, Stanford, California

14

15   **Keywords:** COVID-19, infectiousness, SARS-CoV-2, subgenomic RNA, cohort

16

17   **Abstract Word Count:** 267

18   **Word Count:** 3086

19   **Running title:** sgRNA kinetics in COVID-19 patients

20

21   **Correspondence:**

22   Jason Andrews  
23   Division of Infectious Diseases and Geographic Medicine  
24   Stanford University School of Medicine  
25   Biomedical Innovations Building, Rm 3458  
26   240 Pasteur Dr.  
27   Stanford, CA 94305  
28   Email: [jandr@stanford.edu](mailto:jandr@stanford.edu)  
29   Phone: +1 650 497 2679

30

31

32 **Summary:** We observed prolonged detection of subgenomic RNA in nasal swabs and equivalent  
33 decay rates to genomic RNA in both longitudinal nasal swabs and in remdesivir-treated  
34 A549<sup>ACE2+</sup> cells infected with SARS-CoV-2. Taken together, these findings suggest that  
35 subgenomic RNA from SARS-CoV-2 is comparably stable to genomic RNA and that its  
36 detection is therefore not a more reliable indicator of replicating virus.

37

## 38 **Abstract**

### 39 **Background**

40 Given the persistence of viral RNA in clinically recovered COVID-19 patients, subgenomic  
41 RNAs (sgRNA) have been reported as potential molecular viability markers for SARS-CoV-2.  
42 However, few data are available on their longitudinal kinetics, compared with genomic RNA  
43 (gRNA), in clinical samples.

### 44 **Methods**

45 We analyzed 536 samples from 205 patients with COVID-19 from placebo-controlled, outpatient  
46 trials of Peginterferon Lambda-1a (Lambda; n=177) and favipiravir (n=359). Nasal swabs were  
47 collected at three time points in the Lambda (Day 1, 4 and 6) and favipiravir (Day 1, 5, and 10)  
48 trials. N-gene gRNA and sgRNA were quantified by RT-qPCR. To investigate the decay kinetics  
49 *in vitro*, we measured gRNA and sgRNA in A549<sup>ACE2+</sup> cells infected with SARS-CoV-2,  
50 following treatment with remdesivir or DMSO control.

### 51 **Results**

52 At six days in the Lambda trial and ten days in the favipiravir trial, sgRNA remained detectable  
53 in 51.6% (32/62) and 49.5% (51/106) of the samples, respectively. Cycle threshold (Ct) values  
54 for gRNA and sgRNA were highly linearly correlated (Pearson's  $r=0.87$ ) and the rate of increase  
55 did not differ significantly in Lambda (1.36 cycles/day vs 1.36 cycles/day;  $p = 0.97$ ) or  
56 favipiravir (1.03 cycles/day vs 0.94 cycles/day;  $p=0.26$ ) trials. From samples collected 15-21  
57 days after symptom onset, sgRNA was detectable in 48.1% (40/83) of participants. In SARS-  
58 CoV-2 infected A549<sup>ACE2+</sup> cells treated with remdesivir, the rate of Ct increase did not differ  
59 between gRNA and sgRNA.

### 60 **Conclusions**

61 In clinical samples and *in vitro*, sgRNA was highly correlated with gRNA and did not  
62 demonstrate different decay patterns to support its application as a viability marker.

63

64

## 65 INTRODUCTION

66 Understanding and quantifying the replicating or transcriptionally active virus among individuals  
67 with SARS-CoV-2 could inform treatment decisions and response monitoring, as well as the  
68 need for isolation, contact tracing and infection control measures. The duration of infectiousness  
69 as estimated from transmission studies appears much shorter than the duration of PCR positivity  
70 in airway secretions (1,2). Studies comparing culture and RT-PCR from the same samples have  
71 revealed that there is often substantial discrepancy between these measurements, with PCR  
72 remaining positive for days to weeks longer than culture (3-7). While culture remains the  
73 reference standard for detection of infectious virus, it may lack sensitivity, and it requires  
74 biosafety level 3 facilities, precluding its use at scale as a clinical or public health tool (8). To  
75 overcome this obstacle, there has been considerable interest in the development of molecular  
76 viability markers to sensitively detect and quantify transcriptionally active virus (3,9,10).

77  
78 SARS-CoV-2 is an enveloped, positive sense, single-stranded RNA virus which employs a  
79 complicated pattern of replication as well as transcription of genome length and smaller sgRNAs  
80 (11). These sgRNAs are transcriptional intermediates, susceptible to enzymatic degradation, and  
81 are not believed to be packaged in the final progeny virion, making them an attractive marker for  
82 an actively transcribing virus (12). Small clinical studies have suggested that, compared with  
83 gRNA, sgRNA correlates better with culturable virus. These studies targeted N-gene to detect  
84 gRNA and compared sgRNA stability with a relatively less abundant/sensitive E-gene sgRNA  
85 assay (2,3,9). Despite the E-gene sgRNA assay possibly being suboptimal and may give false  
86 negative results, these findings have led to the use of sgRNA assay as an outcome in preclinical  
87 investigation of novel therapies (13,14) and its suggested use to terminate medical isolation for

88 individuals with COVID-19 (3). In contrast, a recent study found that sgRNAs were detectable  
89 up to 17 days after initial detection and that they may be protected from nuclease degradation by  
90 double membrane vesicles (15). However, because this study only had 12 clinical samples,  
91 further evidence about the kinetics of sgRNA versus gRNA in longitudinal samples is needed to  
92 determine whether sgRNA abundance better reflects recently transcribing viral infection.  
93 Additionally, in order to serve as a marker of replicating virus, sgRNA is expected to show a  
94 rapid decline after transcriptional inhibition due to ribonuclease degradation, in contrast to  
95 gRNA, which may be protected from degradation by viral capsids and therefore persist more  
96 durably (16). Therefore, we hypothesized that, upon treatment with SARS-CoV-2 RNA-  
97 dependent RNA polymerase inhibitors (17, 18, 19) in cell lines infected with SARS-CoV-2, we  
98 should observe a rapid decline of sgRNA after viral death when compared with gRNA.

99  
100 To address these gaps, we developed an N-gene sgRNA assay to directly compare its stability  
101 with N-gene gRNA. sgRNAs in SARS-CoV-2 share a common leader sequence at the 5' end  
102 which is absent in the gene amplified from the gRNA (9). We combined the common leader  
103 sequence as forward primer with CDC N1 gene assay's reverse primer (20) to facilitate  
104 comparison of N-gene sgRNA with gRNA copies. We applied this assay to serial samples from  
105 individuals participating in two randomized clinical trials to characterize decay rates.  
106 Additionally, we leveraged the inhibition of viral transcription and replication by an RNA-  
107 dependent RNA polymerase inhibitor (remdesivir) (19) to measure and compare the decay  
108 kinetics of gRNA and sgRNA following polymerase inhibition in SARS-CoV-2 infected  
109 A549<sup>ACE2+</sup> cells.

110

## 111 **METHODS**

112

### 113 **Ethics statement**

114 All participants were >18 years of age and provided written informed consent. The studies were  
115 approved by the Stanford IRB (#57686 and #58869).

116

### 117 **Overview and Study Population**

118 This was a sub-study of two Phase 2 randomized, placebo-controlled trials of peginterferon-  
119 Lambda-1a (Lambda) (NCT04331899) and favipiravir (NCT04346628) for treatment of  
120 COVID-19. Individuals >18 years of age with RT-PCR confirmed SARS-CoV-2 infection were  
121 recruited to participate and were eligible if they could be randomized within 72 hours of a  
122 positive SARS-CoV-2 test and were not hospitalized. Additional exclusion criteria were  
123 respiratory rate < 20 breaths per minute, room air oxygen saturation <94%, pregnancy or  
124 breastfeeding, or use of other investigational agents for treatment of COVID-19. In the Lambda  
125 trial, enrolled participants were randomized to a single injection with 180 mcg of Lambda versus  
126 placebo injection and followed for 28 days. In the favipiravir trial, individuals were randomized  
127 to oral favipiravir tablets (1800 mg on day 1, followed by 800 mg twice daily for 9 days) or  
128 matching placebo. The primary outcome for both studies was time to cessation of viral shedding  
129 as measured by qRT-PCR performed on oropharyngeal swab samples (Lambda trial) or nasal  
130 swabs (favipiravir trial). In August 2020, we amended both protocols to collect nasal swabs (LH-  
131 11-10 Longhorn Hydra Sterile Flocked Swab) to assay for gRNA and sgRNA. For Lambda trial,  
132 it was earlier found that in both patients receiving Lambda and placebo, the median time to  
133 cessation of viral shedding was 7 days (21). A single dose of subcutaneous Peginterferon

134 Lambda-1a neither shortened the duration of SARS-CoV-2 viral shedding nor improved  
135 symptoms in outpatients (21). The favipiravir trial is an ongoing study and remains blinded.

136

### 137 **RNA extraction and quantitative RT-PCR assay for SARS-CoV-2 RNA**

138 Nasal swabs were collected and transported in 500 ul of Primestore MTM (Longhorn Vaccines  
139 & Diagnostics) RNA stabilizing media. RNA was extracted using MagMAX™ Viral/Pathogen  
140 Ultra Nucleic Acid Isolation Kit (Cat # A42356 Applied Biosystems) according to the  
141 manufacturer's instructions and eluted in 50ul of elution buffer. We performed qRT-PCR for the  
142 N gene using the CDC qualified primers and probes amplifying N1 region of SARS-CoV-2 N-  
143 gene (20). TaqPath one-step RT-PCR mastermix (Invitrogen, Darmstadt, Germany) was used in  
144 a 20ul reaction volume and the samples were analyzed on a StepOne-Plus (Applied Biosystems)  
145 instrument, using the following program: 10 min at 50 °C for reverse transcription, followed by 3  
146 min at 95 °C and 40 cycles of 10 s at 95 °C, 15 s at 56 °C, and 5 s at 72 °C. We estimated  
147 copies/sample from a standard curve using a pET21b+ plasmid (GenScript, USA) with the N-  
148 gene. The cycle threshold (Ct) cutoff for positive samples was <38.

149

### 150 **Quantitative RT-PCR Assay for SARS-CoV-2 sgRNA**

151 Since all sgRNAs are known to carry a common leader sequence, to amplify N-gene sgRNA, we  
152 combined a previously described E-gene sgRNA forward primer for SARS-CoV-2 leader  
153 sequence along with the CDC N1-gene segment reverse primer and probe to detect N-gene  
154 sgRNA (3). We used TaqPath one-step RT-PCR mastermix with 400 nM concentrations of each  
155 of the primer and 200 nM of probe to amplify sgRNA. The N-gene PCR reactions conditions  
156 were used for sgRNA amplification. We estimated copies/sample from a standard curve using a



157 pET21b+ plasmid with the N-gene sgRNA sequence. The cycle threshold (Ct) cutoff for positive  
158 samples was <38.

159

### 160 **sgRNA validation by Sanger sequencing**

161 For the first 15 positive clinical samples, we confirmed amplification product identity by Sanger  
162 sequencing. We performed endpoint PCR using the same primers, purified it by gel  
163 electrophoresis, and performed Sanger sequencing with these primers. The resulting sequences  
164 were aligned using to SARS-CoV-2 genome (GenBank: MT568638.1) to compare sequence  
165 similarity of the product with the leader sequence and N-gene. Samples were considered positive  
166 for sgRNA if the leader sequence identity with the reference genome was greater than 98%.

167

### 168 **sgRNA kinetics in SARS-CoV-2 infected A549<sup>ACE2+</sup> cells**

169 *Cell culture and in vitro SARS-CoV-2 infection:*

170 The human lung epithelial carcinoma cell line, A549, overexpressing Angiotensin-converting  
171 enzyme 2 (ACE2), A549<sup>ACE2+</sup>, was provided by Ralf Bartenschlager (Heidelberg University)  
172 (22). A549<sup>ACE2+</sup> cells were cultured in Dulbecco's Modified Eagle Medium (DMEM) (Life  
173 technologies; 11885-092) supplemented with 10% Fetal bovine serum (Corning; MT35016CV),  
174 1% Penicillin-Streptomycin (Thermo Fisher Scientific; 15070063), and 623ug/ml of Geneticin  
175 (Thermo Fisher Scientific; 10121035). For viral infection, cells were seeded a day before  
176 infection by culturing  $1 \times 10^5$  cells per well in a 6-well plate (Corning). Cells were at passage 14  
177 at the time of infection. Viral infection was performed with the Washington strain of SARS-  
178 CoV-2 (2019-nCoV/USA-WA1/2020), titered by plaque assay on VeroE6 cells, at a multiplicity  
179 of infection (MOI) of 1. Briefly, in Biosafety level 3 (BSL3) containment, culture media was

180 removed, and cells were washed with phosphate buffered saline (PBS) (Thermo Fisher  
181 Scientific; 10-296-028) multiple times before adding the viral stock. Cells were then incubated at  
182 37°C with 5% CO<sub>2</sub> for 1 hour while gently rocking. After 1 hour, cells were washed with 1x PBS  
183 and incubated in culture media. Supernatant and cells were collected at 1 and 24 hours post-  
184 infection (hpi) in TRIzol LS (Thermo Fisher Scientific; 10010023) for RNA extraction. Other  
185 wells were either treated with 0.1% final concentration of dimethylsulfoxide (DMSO) (Sigma  
186 Life Science: Cat# D2650) or 10µM remdesivir (Gilead, Cat# NDC 61958-2901-2) in 0.1%  
187 DMSO and cultured for longer periods (48, 72, and 96hpi). It has been previously demonstrated  
188 that at 10µM prodrug concentration, remdesivir potently inhibits SARS-CoV-2 in A549<sup>ACE2+</sup>  
189 cells (23). Cytopathic effect on SARS-CoV-2 in vitro-infected A549<sup>ACE2+</sup> cells that were treated  
190 with either 10µM remdesivir or vehicle, 0.1% DMSO, was monitored before and after infection.  
191 Cell line experiments at all time-points and treatment conditions were performed in technical  
192 duplicates. Cells and supernatant were collected, and RNA was extracted independently for all  
193 technical duplicates without pooling. An image of cells was collected using an EVOS XL core  
194 imaging system (Thermo Fisher scientific), with a 10x objective, before collecting cell pellet and  
195 supernatant from each treatment, and time point.

196

#### 197 *RNA extraction and RT-PCR*

198 RNA from supernatant and cells collected at 1, 24, 48, 72 and 96 hpi in TRIzol LS was extracted  
199 using isolated using standard phenol-chloroform extraction per manufacturer's instructions. The  
200 SARS-CoV-2 genomic and sgRNA RT-qPCR assays from cell line technical duplicates were  
201 further performed in technical duplicates. The RNA copies were quantified using standard curves

202 derived from plasmids. Eukaryotic 18S rRNA commercial TaqMan assay (4333760T, Thermo  
203 Fisher Scientific) was used as an internal control.

204

## 205 **Statistical Analyses**

206 We estimated the change in cycle threshold (Ct) value for gRNA and sgRNA by day using  
207 generalized linear mixed models with random effect for participant. We tested for differences in  
208 the coefficients for collection day for outcomes of gRNA and sgRNA by performing ANOVA on  
209 a joint model with a dummy variable for RNA type. We used generalized additive mixed models  
210 with a random effect for participant to investigate the relationship between sample collection day  
211 and cycle threshold (Ct) values. All analyses were performed using R (24).

212

## 213 **RESULTS**

### 214 **Study population characteristics**

215 We recruited 205 COVID-19 positive patients from placebo-controlled trials of interferon  
216 Lambda (n=66) and Favipiravir (n=139) between August, 2020 and January, 2021. All  
217 participants were enrolled in the trials within 72 hours of a positive SARS-CoV-2 RT-qPCR test.  
218 Median age of the participants was 40 years (range, 18-73), and 46.8% (96/205) were female.  
219 The majority of participants (197/205; 96.1%) reported one or more COVID-19 related  
220 symptoms several days prior to enrollment (median, 5 days; range, 0-21). Symptoms with onset  
221 more than three weeks prior to study enrollment were not considered to be associated with  
222 COVID-19. The most common baseline symptoms reported by the patients before randomization  
223 were cough, diarrhea, body ache, headache, fatigue and shortness of breath (Table 1).

224

## 225 **gRNA and sgRNA RT-qPCR positivity in clinical samples**

226 We analyzed 536 nasal swab samples collected from 205 COVID-19 patients from the Lambda  
227 (n=177) and favipiravir (n=359) trials between 0 to 21 days post symptom onset. For the  
228 favipiravir trial, nasal swabs were collected on the day of enrollment (day 1), followed by day 5  
229 and day 10. For Lambda trial, nasal swabs were collected on the day of enrollment (day 1)  
230 followed by day 4 and day 6. Overall gRNA RT-qPCR positivity in samples from the favipiravir  
231 trial on day 1, 5 and 10 was 91.5%, 82.9% and 60.3% respectively (Table 2). For sgRNA,  
232 positivity was 89.2%, 77.2% and 49.5%. For the Lambda trial, overall gRNA positivity on day 1,  
233 4 and 6 was 91.6%, 90.9% and 91.9% respectively. For sgRNA, overall positivity was 81.6%,  
234 74.5% and 51.6%. We observed a high correlation (Pearson's  $r=0.87$ ) between the cycle  
235 threshold (Ct) values of gRNA and sgRNA at all time points, and detection of sgRNA was  
236 strongly predicted by gRNA Ct (**Figure 1**). For the first 15 samples for which sgRNA showed  
237 positive amplification, we performed Sanger sequencing. All fifteen samples had more than 98%  
238 identity with SARS-CoV-2 leader sequence, confirming amplification of the sgRNA transcript  
239 (Supplementary figure 1). In a subset of 35 samples in which we performed testing for E-gene  
240 sgRNA using a previously published assay, we found high correlation (Pearson's  $r=0.89$ ) with  
241 N-gene sgRNA, but with higher Ct values (median difference, 4.1 cycles) among positive  
242 samples. Among 35 samples positive for N-gene sgRNA, 69.0% (24/35) were negative for E-  
243 gene sgRNA (Supplementary figure 2).

244

245 Randomization data was available for the Lambda study while favipiravir still remains blinded.

246 We did not observe any significant difference in the Ct values of sgRNA between Lambda and  
247 placebo recipients. At day six, the gRNA percentage positivity was 83.8% (26/31) (median Ct

248 value = 32.5) in Lambda and 100% (31/31) (median Ct value =33.4) in placebo arm. In sgRNA  
249 at day six, percentage positivity was 48.3% (15/31) (median Ct value = 38.0) in Lambda and  
250 54.8% (17/31) (median Ct value =35.9) in placebo arm (p=0.903).

251  
252 We found no difference in the rate of Ct value increase by day in gRNA compared with sgRNA  
253 in the Lambda (1.36 cycles/day vs 1.36 cycles/day; p=0.97) or favipiravir (1.03 cycles/day vs  
254 0.94 cycles/day; p=0.26) trials (Figure 2). Among samples collected 15-21 days after symptom  
255 onset from both trials combined, sgRNA was detectable in 48.1% (40/83) of participants (Figure  
256 3).

#### 257 258 **sgRNA kinetics in SARS-CoV-2 infected A549<sup>ACE2+</sup> cells treated with remdesivir**

259 We compared SARS-CoV-2 gRNA and sgRNA degradation kinetics after transcriptional  
260 inhibition by antiviral drug remdesivir. We treated SARS-CoV-2 infected A549<sup>ACE2+</sup> cells with  
261 0.1% DMSO vehicle control and 10 $\mu$ M remdesivir at 24hpi. Cytopathic effects were observed in  
262 cells treated with DMSO control but not remdesivir (Supplementary figure 3). Compared with  
263 DMSO treated cells, SARS-CoV-2 replication in remdesivir treated cells was markedly reduced  
264 (nadir gRNA Ct 9.6 vs 14.2; nadir sgRNA Ct 10.0 vs 14.5). In remdesivir-treated cells, gRNA  
265 and sgRNA Ct values rose at similar rates in cells (0.11/hour vs 0.09/hour; p=0.153) and  
266 declined by similar rates in supernatant (-0.06/hour vs 0.06/hour; p=0.914) (Figure 4).

267

268

## 269 **DISCUSSION**

270 While there has been considerable interest in the use of sgRNAs as markers of replicating SARS-  
271 CoV-2 infection, evidence concerning the decay of sgRNA following onset of infection in  
272 humans and cell culture has been lacking. Using longitudinal samples from two clinical trials, we  
273 found that sgRNA was detectable in 46% of participants from the Lambda trial and 50% from  
274 favipiravir trial 15-21 days after symptoms onset. While gRNA was detectable for longer than  
275 sgRNA, they were highly correlated and had indistinguishable rates of decline within individuals  
276 over time. We found consistent results in cell culture, whereby gRNA and sgRNA copies  
277 declined at the same rate following inhibition of transcription by remdesivir. Taken together,  
278 these findings suggest that detection of sgRNAs is not a reliable marker of recent viral  
279 transcription and does not provide marginal information over quantification of gRNA. Earlier  
280 findings of greater specificity of sgRNAs than gRNAs compared with a reference standard of  
281 culture may be explained by the lower analytical sensitivity of the sgRNA assays (3,9,10),  
282 particularly using less sensitive E-gene assays.

283  
284 RNA transcripts have been used as markers of viability or metabolic activity for a number of  
285 bacterial and viral pathogens. In bacteria, mRNAs have much shorter half-lives than DNA due to  
286 degradation by ribonucleases, such that their presence indicates recent metabolic activity  
287 (25,26,27). Similarly, RNA transcription assays have been used to assess replication competent  
288 viral pool size for HIV-1 (28). For SARS-CoV-2, sgRNA transcription is believed to occur  
289 inside double membrane vesicles, which may protect viral genomic and subgenomic RNA from  
290 cytoplasmic degradation due to host enzymes (29-33). We found that sgRNA and gRNA  
291 increased at the same rate following infection of cells and then declined at the same rate

292 following cell death (in the control cells treated with DMSO) or following inhibition of RDRP  
293 (RNA dependent RNA polymerase) by remdesivir. If sgRNAs were rapidly degraded by  
294 ribonucleases, we would have expected a more rapid decline in sgRNAs compared with gRNAs,  
295 but this was not observed. Similarly, in the supernatant, we saw no difference in change in  
296 sgRNAs compared with gRNAs, again failing to identify rapid clearance of sgRNAs by  
297 ribonucleases.

298  
299 Several previous studies have targeted E-gene sgRNA, reporting in small clinical series that  
300 these correlated well with culture (34, 35). This finding may be explained by the fact that E-gene  
301 transcripts are less abundant than N-gene transcripts, so assays targeting them will have lower  
302 analytical sensitivity (36). Indeed, we performed direct comparison of N-gene and E-gene assays  
303 and found that the latter were approximately 5 Ct values higher for the same sample. There is not  
304 clear premise to infer that E-gene transcripts are more rapidly degraded by ribonucleases or that  
305 they better reflect recent transcription than N-gene sgRNAs. Negative-strand RNA detection in  
306 SARS-CoV-2 has recently been reported as another potential viability marker (37). In a study by  
307 Alexanderson and group, negative strand RNA was detected up to 11 days (15). However,  
308 negative strand assays may be less analytically sensitive than sgRNA assays (37). This could  
309 make them appear to be more specific, compared with culture, in clinical samples as they are  
310 more likely to be negative when viral abundance is low.

311  
312 Our study has several limitations, which include lack of viral culture data and samples at later  
313 timepoints. Additionally, to study the sgRNA decay kinetics, we targeted a single and highly  
314 abundant gene to compare and quantify gRNA and sgRNA, though we found high correlation

315 between E-gene and N-gene sgRNA copy numbers. Analyzing additional targets would help us  
316 understand the stability of other sgRNAs. Another limitation our study is lack of unblinded data  
317 from the favipiravir study, precluding analysis by study arm. However, our findings of sgRNA  
318 persistence in clinical samples and lack of difference in its decline compared with gRNA are  
319 notable regardless of whether favipiravir reduced levels in one arm. For remdesivir, a RDRP  
320 inhibitor like favipiravir, we found no differential effect on sgRNA, compared with gRNA, in  
321 cell culture, despite effective reduction in viral replication and cytopathic effects.

322  
323 In summary, we found that SARS-CoV-2 sgRNAs are persistently detectable in clinical samples,  
324 correlate strongly with gRNA, and decline at indistinguishable rates in clinical samples and cell  
325 culture. We find little evidence to support the premise that sgRNA detection is a reliable marker  
326 of transcriptionally active virus or that it provides additional information beyond detection of  
327 gRNA in clinical samples. We advise caution against using sgRNA assays to inform decisions  
328 concerning treatment or medical isolation.

329



330 **Funding**

331 This study was funded by Bill Gates and Melinda Gates Foundation (OPP1113682 – Stanford  
332 Center for Human Systems Immunology). The parent clinical trials from which the clinical  
333 samples were collected were supported by Stanford’s Innovative Medicines Accelerator and by  
334 Stanford ChEM-H.

335

336 **Acknowledgements**

337 We thank the study teams and participants of the Lambda and favipiravir clinical trials. SARS-  
338 Related Coronavirus 2, Isolate USA-WA1/2020, NR-52281 was deposited by the CDC and  
339 obtained through BEI Resources, NIAID, NIH. We thank Jaishree Garhyan, Director, Invitro  
340 BSL-3 Service Center, Stanford School of Medicine.

341

342 **Author contributions**

343 JRA and RV conceived the idea of the study. JRA, RV, GMC and CB designed the experiments.  
344 PJ, HB, US, AS, MH, YM, and JRA enrolled the clinical cohorts. RV, EK, and GMC performed  
345 the experiments. JRA, RV and EK analyzed data. RV and JRA wrote the first draft of the  
346 manuscript, and all authors contributed to the final version.

347

348 **Conflicts of Interest**

349 We declare that we have no conflicts of interest for this work.

350

351

352

353

354 **References:**

- 355 1. He X, Lau EHY, Wu P, et al. Temporal dynamics in viral shedding and transmissibility  
356 of COVID-19. *Nat Med.* 2020 May;26(5):672-675.
- 357 2. Kim MC, Cui C, Shin KR, et al. Duration of Culturable SARS-CoV-2 in Hospitalized  
358 Patients with Covid-19. *N Engl J Med.* 2021 Feb 18;384(7):671-673.
- 359 3. Wölfel R, Corman VM, Guggemos W, et al. Virological assessment of hospitalized  
360 patients with COVID-2019. *Nature.* 2020 May;581(7809):465-469
- 361 4. Mallett S, Allen AJ, Graziadio S, et al. At what times during infection is SARS-CoV-2  
362 detectable and no longer detectable using RT-PCR-based tests? A systematic review of  
363 individual participant data. *BMC Med.* 2020 Nov 4;18(1):346.
- 364 5. Bullard J, Dust K, Funk D, Strong JE, et al. Predicting infectious SARS-CoV-2 from  
365 diagnostic samples. *Clin Infect Dis.* 2020 May 22:ciaa638.
- 366 6. COVID-19 Investigation Team. Clinical and virologic characteristics of the first 12  
367 patients with coronavirus disease 2019 (COVID-19) in the United States. *Nat Med.* 2020  
368 Jun;26(6):861-868.
- 369 7. Singanayagam A, Patel M, Charlett A, et al. Duration of infectiousness and correlation  
370 with RT-PCR cycle threshold values in cases of COVID-19, England, January to May  
371 2020. *Euro Surveill.* 2020 Aug;25(32):2001483.
- 372 8. Jafari H, Amiri Gharaghani M. Cultural Challenges: The Most Important Challenge of  
373 COVID-19 Control Policies in Iran. *Prehosp Disaster Med.* 2020 Aug;35(4):470-471.
- 374 9. Perera RAPM, Tso E, Tsang OTY, et al. SARS-CoV-2 Virus Culture and Subgenomic  
375 RNA for Respiratory Specimens from Patients with Mild Coronavirus Disease. *Emerg*  
376 *Infect Dis.* 2020 Nov;26(11):2701-2704.

- 377 10. Williamson BN, Feldmann F, Schwarz B, et al. Clinical benefit of remdesivir in rhesus  
378 macaques infected with SARS-CoV-2. *Nature*. 2020 Sep;585(7824):273-276.
- 379 11. Sola I, Almazán F, Zúñiga S, Enjuanes L. Continuous and Discontinuous RNA Synthesis  
380 in Coronaviruses. *Annu Rev Virol*. 2015 Nov;2(1):265-88.
- 381 12. Wu HY, Brian DA. Subgenomic messenger RNA amplification in coronaviruses. *Proc*  
382 *Natl Acad Sci U S A*. 2010 Jul 6;107(27):12257-62.
- 383 13. Corbett KS, Flynn B, Foulds KE, et al. Evaluation of the mRNA-1273 Vaccine against  
384 SARS-CoV-2 in Nonhuman Primates. *N Engl J Med*. 2020 Oct 15;383(16):1544-1555.
- 385 14. van Doremalen N, Lambe T, Spencer A, et al. ChAdOx1 nCoV-19 vaccine prevents  
386 SARS-CoV-2 pneumonia in rhesus macaques. *Nature*. 2020 Oct;586(7830):578-582.
- 387 15. Alexandersen S, Chamings A, Bhatta TR. SARS-CoV-2 genomic and subgenomic RNAs  
388 in diagnostic samples are not an indicator of active replication. *Nat Commun*. 2020 Nov  
389 27;11(1):6059.
- 390 16. Cliver DO. Capsid and Infectivity in Virus Detection. *Food Environ Virol*. 2009 Dec;1(3-  
391 4):123-128.
- 392 17. Yin W, Luan X, Li Z, Zhou Z, Wang Q, Gao M, Wang X, Zhou F, Shi J, You E, Liu M,  
393 Wang Q, Jiang Y, Jiang H, Xiao G, Zhang L, Yu X, Zhang S, Eric Xu H. Structural basis  
394 for inhibition of the SARS-CoV-2 RNA polymerase by suramin. *Nat Struct Mol Biol*.  
395 2021 Mar;28(3):319-325.
- 396 18. Naydenova K, Muir KW, Wu LF, Zhang Z, Coscia F, Peet MJ, Castro-Hartmann P, Qian  
397 P, Sader K, Dent K, Kimanius D, Sutherland JD, Löwe J, Barford D, Russo CJ. Structure  
398 of the SARS-CoV-2 RNA-dependent RNA polymerase in the presence of favipiravir-  
399 RTP. *Proc Natl Acad Sci U S A*. 2021 Feb 16;118(7)

- 400 19. Kokic G, Hillen HS, Tegunov D, Dienemann C, Seitz F, Schmitzova J, Farnung L,  
401 Siewert A, Höbartner C, Cramer P. Mechanism of SARS-CoV-2 polymerase stalling by  
402 remdesivir. *Nat Commun.* 2021 Jan 12;12(1):279.
- 403 20. <https://www.cdc.gov/coronavirus/2019-ncov/lab/rt-pcr-panel-primer-probes.html>
- 404 21. Jagannathan P, Andrews JR, Bonilla H, et al. Peginterferon Lambda-1a for treatment of  
405 outpatients with uncomplicated COVID-19: a randomized placebo-controlled trial. *Nat*  
406 *Commun.* 2021 Mar 30;12(1):1967.
- 407 22. Klein S, Cortese M, Winter SL, et al. SARS-CoV-2 structure and replication  
408 characterized by in situ cryo-electron tomography. *Nat Commun.* 2020 Nov  
409 18;11(1):5885.
- 410 23. de Vries M, Mohamed AS, Prescott RA, et al. A comparative analysis of SARS-CoV-2  
411 antivirals characterizes 3CL<sup>pro</sup> inhibitor PF-00835231 as a potential new treatment for  
412 COVID-19. *J Virol.* 2021 Feb 23;JVI.01819-20.
- 413 24. R Core Team (2014). R: A language and environment for statistical computing. R  
414 Foundation for Statistical  
415 Computing, Vienna, Austria. URL <http://www.R-project.org/>
- 416 25. Cenciarini-Borde C, Courtois S, La Scola B. Nucleic acids as viability markers for  
417 bacteria detection using molecular tools. *Future Microbiol.* 2009 Feb;4(1):45-64.
- 418 26. Nocker A, Camper AK. Novel approaches toward preferential detection of viable cells  
419 using nucleic acid amplification techniques. *FEMS Microbiol Lett.* 2009 Feb;291(2):137-  
420 42.
- 421 27. NEIDHARDT FC, MAGASANIK B. Studies on the role of ribonucleic acid in the  
422 growth of bacteria. *Biochim Biophys Acta.* 1960 Jul 29;42:99-116.

- 423 28. Plantin J, Massanella M, Chomont N. Inducible HIV RNA transcription assays to  
424 measure HIV persistence: pros and cons of a compromise. *Retrovirology*. 2018 Jan  
425 17;15(1):9.
- 426 29. Escors D, Izeta A, Capiscol C, et al. Transmissible gastroenteritis coronavirus packaging  
427 signal is located at the 5' end of the virus genome. *J Virol*. 2003 Jul;77(14):7890-902.
- 428 30. Snijder EJ, Limpens RWAL, de Wilde AH, et al. A unifying structural and functional  
429 model of the coronavirus replication organelle: Tracking down RNA synthesis. *PLoS*  
430 *Biol*. 2020 Jun 8;18(6):e3000715.
- 431 31. Wolff G, Limpens RWAL, Zevenhoven-Dobbe JC, et al. A molecular pore spans the  
432 double membrane of the coronavirus replication organelle. *Science*. 2020 Sep  
433 11;369(6509):1395-1398.
- 434 32. Wada M, Lokugamage KG, Nakagawa K, et al. Interplay between coronavirus, a  
435 cytoplasmic RNA virus, and nonsense-mediated mRNA decay pathway. *Proc Natl Acad*  
436 *Sci U S A*. 2018 Oct 23;115(43):E10157-E10166.
- 437 33. Wu HY, Brian DA. Subgenomic messenger RNA amplification in coronaviruses. *Proc*  
438 *Natl Acad Sci U S A*. 2010 Jul 6;107(27):12257-62.
- 439 34. Perera RAPM, Tso E, Tsang OTY, et al. SARS-CoV-2 Virus Culture and Subgenomic  
440 RNA for Respiratory Specimens from Patients with Mild Coronavirus Disease. *Emerg*  
441 *Infect Dis*. 2020 Nov;26(11):2701-2704.
- 442 35. Williamson BN, Feldmann F, Schwarz B, et al. Clinical benefit of remdesivir in rhesus  
443 macaques infected with SARS-CoV-2. *Nature*. 2020 Sep;585(7824):273-276.
- 444 36. Kim D, Lee JY, Yang JS, et al. The Architecture of SARS-CoV-2 Transcriptome. *Cell*.  
445 2020 May 14;181(4):914-921.e10.

446 37. Hogan CA, Huang C, Sahoo MK, et al. Strand-Specific Reverse Transcription PCR for  
447 Detection of Replicating SARS-CoV-2. *Emerg Infect Dis.* 2021 Feb;27(2):632-635.  
448  
449  
450  
451  
452

453 **Figures**

454

455 **Figure 1: Correlation between genomic and subgenomic RNA in clinical samples. (A)**

456 Genomic and sgRNA Ct values from clinical samples showed strong correlation (Pearson's  $r=$   
457 0.87). Dashed line reflects the diagonal of equal cycle thresholds, and solid line is the best fit  
458 regression line with shaded area indicating the 95% confidence interval. **(B)** Detection of sgRNA  
459 was predicted by cycle threshold value of gRNA.

460

461 **Figure 2: Cycle threshold values for genomic and subgenomic RNA by sample collection**

462 **day.** Boxplot representing Ct values for genomic (Purple) and sgRNA (Blue) from serially  
463 collected COVID-19 samples. **(A)** N-gene genomic and sgRNA decay trend in samples from the  
464 Lambda trial collected at day 1, 4 and 6. **(B)** N-gene genomic and sgRNA decay trend in samples  
465 from the favipiravir trial collected at day 1, 5 and 10.

466

467 **Figure 3: Proportion of samples positive for genomic and subgenomic RNA from time of**

468 **symptom onset.** Samples from the Lambda and favipiravir trials were combined, and a positive  
469 sample was one with cycle threshold  $<38$ . Error bars denote 95% exact binomial confidence  
470 intervals.

471

472 **Figure 4: SARS-CoV-2 genomic and subgenomic RNA kinetics in cell culture. SARS-CoV-2**

473 genomic and sgRNA kinetics in A549<sup>ACE2+</sup> cells treated with 0.1% DMSO and 10 $\mu$ M remdesivir  
474 (RDV). Solid lines indicate genomic (Purple) and sgRNA (Blue) levels in A549<sup>ACE2+</sup> cells  
475 treated with remdesivir. Dotted lines indicate genomic (Purple) and sgRNA (Blue) levels in cells

476 treated with 0.1% DMSO. (A) Corresponds to genomic and sgRNA degradation kinetics in  
477 washed cell pellets from A549<sup>ACE2+</sup> cell line. (B) Corresponds to genomic and sgRNA  
478 degradation kinetics in supernatant from A549<sup>ACE2+</sup> cell line.

479

480 **Supplementary Figure 1: (A) Sanger sequencing validation: SARS-CoV-2 sgRNA RT-PCR**

481 results confirmed on Sanger sequencing. The samples were mapped to SARS-CoV-2 genome  
482 (GenBank: MT568638.1) using MUSCLE (MUltiple Sequence Comparison by Log-  
483 Expectation). Clinical samples assayed for sgRNA mapped to the leader sequence and N-gene.

484 **(B)** Schema on sgRNA synthesis in SARS-CoV-2. In full-length genomic RNA, the 5' terminal  
485 contains a leader sequence (yellow). During viral transcription, leader sequence independently  
486 fuses with different genes, resulting in smaller sgRNAs containing a common leader sequence.

487

488 **Supplementary Figure 2: Boxplot representing Ct values for N-gene sgRNA (Blue) and E-gene**

489 sgRNA (Pink). Higher Ct values were observed for the E-gene sgRNA among the samples tested  
490 positive for N-gene sgRNA. A large fraction of samples 69% (24/35), which were positive for N-  
491 gene sgRNA were negative for E-gene sgRNA suggesting poor assay sensitivity.

492

493 **Supplementary Figure 3: Cytopathic effect of SARS-CoV-2 on A549<sup>ACE2+</sup> cells treated with**

494 either 10 $\mu$ M remdesivir or 0.1% DMSO. The images were collected using an EVOS XL core  
495 imaging system (Thermo Fisher scientific), with a 10x objective, before collecting cell pellet and  
496 supernatant from each treatment and time point. Cytopathic effect was characterized by

497 significant changes in morphology from well-spread epithelial cells to small rounded cells, the  
498 inability to achieve confluency, and presence of excessive and unusual rounded floating cells, a



499 characteristic of cell death. (A) Remdesivir treated A549<sup>ACE2+</sup> cells 24hours after treatment at  
500 48hpi (B) DMSO treated A549<sup>ACE2+</sup> cells 24hours after treatment at 48hpi (C) Remdesivir treated  
501 A549<sup>ACE2+</sup> cells 48hours after treatment at 72hpi (D) DMSO treated A549<sup>ACE2+</sup> cells 48hours after  
502 treatment at 72hpi (E) Remdesivir treated A549<sup>ACE2+</sup> cells 72hours after treatment at 96hpi (F)  
503 DMSO treated A549<sup>ACE2+</sup> cells 72hours after treatment at 96hpi.

504

505

506

507  
508  
509  
510

**Table 1: Characteristics of the study participants recruited from the Lambda and favipiravir trials.**

	Trial		
	Lambda (n=66)	Favipiravir (n=139)	Overall (n=205)
<b>Age in years, median (IQR)</b>	36 (31-48.5)	42 (33-53)	40 (32-52)
<b>Female, n (%)</b>	28 (47.5%)	60 (46.2%)	88 (46.6%)
<b>Symptomatic at enrollment, n (%)</b>	66 (100%)	131 (94.2%)	197 (96.1%)
<b>Duration of symptoms prior to enrollment, days, median (IQR)</b>	5 (4-7.75)	5 (3-7)	5 (3-7)
0-7 days, n (%)	49 (74.2%)	110 (79.1%)	159 (77.6%)
8-14 days, n (%)	14 (21.2%)	20 (14.4%)	34 (16.6%)
15-21 days, n (%)	3 (4.5%)	1 (0.7%)	4 (2.0%)

511

512 **Table 2: Genomic and sgRNA RT-qPCR positivity in longitudinal samples from the**  
 513 **Lambda and favipiravir trials.**

<b>Longitudinal swab samples from Lambda clinical trial (n=177)</b>						
	<b>Day 1</b>		<b>Day 4</b>		<b>Day 6</b>	
	Positive, n (%)	Median Ct	Positive (%)	Median Ct	Positive (%)	Median Ct
<b>gRNA</b>	55/60 (91.6%)	24.4	50/55 (90.9%)	30.2	57/62 (91.9%)	33.2
<b>sgRNA</b>	49/60 (81.6%)	26.9	41/55 (74.5%)	32.3	32/62(51.6%)	37.3
<b>Longitudinal swab samples from favipiravir clinical trial (n=359)</b>						
	<b>Day 1</b>		<b>Day 5</b>		<b>Day 10</b>	
	Positive (%)	Median Ct	Positive (%)	Median Ct	Positive (%)	Median Ct
<b>gRNA</b>	119/130 (91.5%)	23.8	102/123 (82.9%)	29.4	64/106 (60.3%)	34.4
<b>sgRNA</b>	116/130 (89.2%)	25.4	95/123 (77.2%)	31.0	51/106 (49.5 %)	38

514

515 Ct cutoff value for positive samples <38; Ct: cycle threshold

516

517

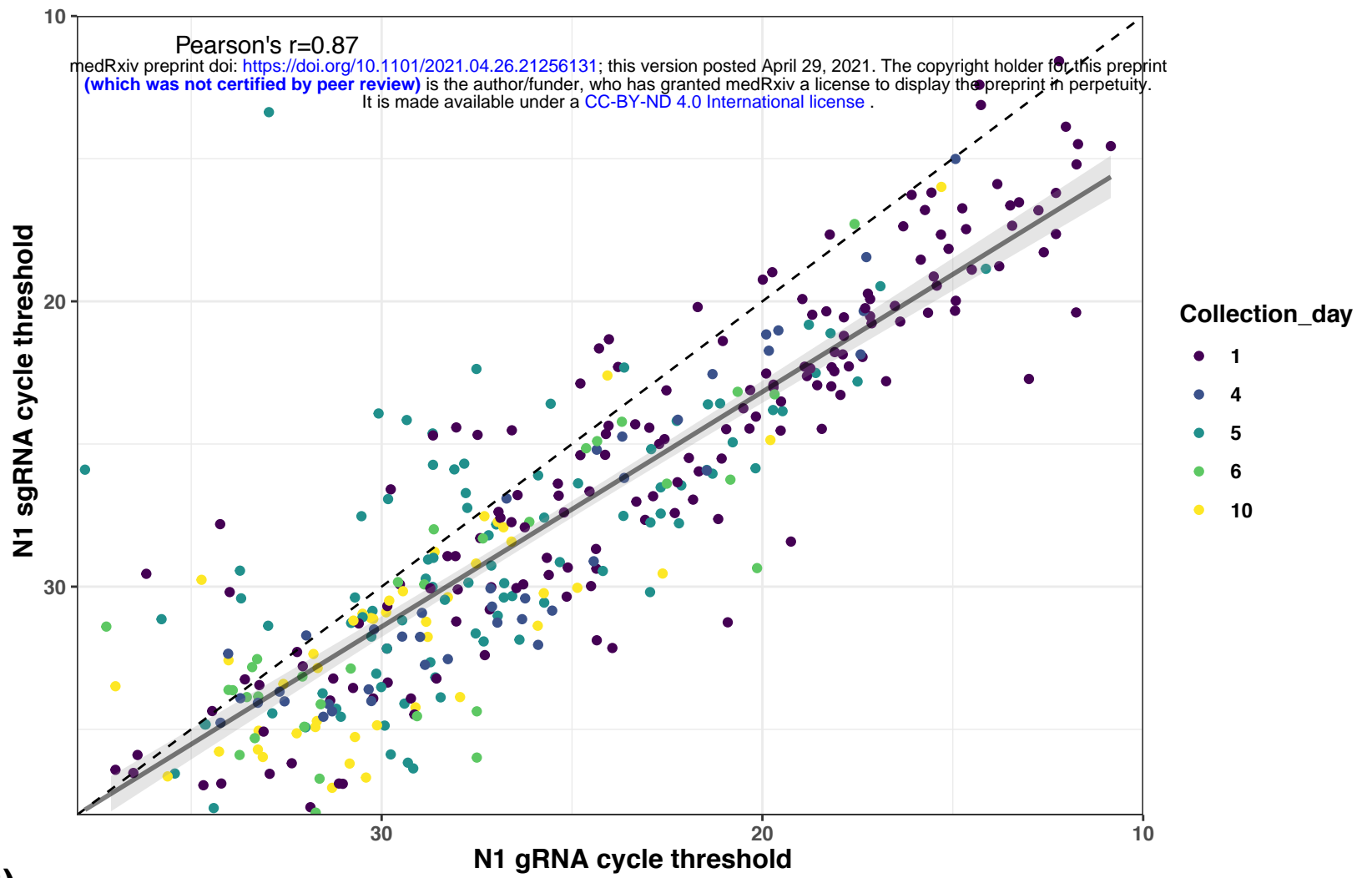
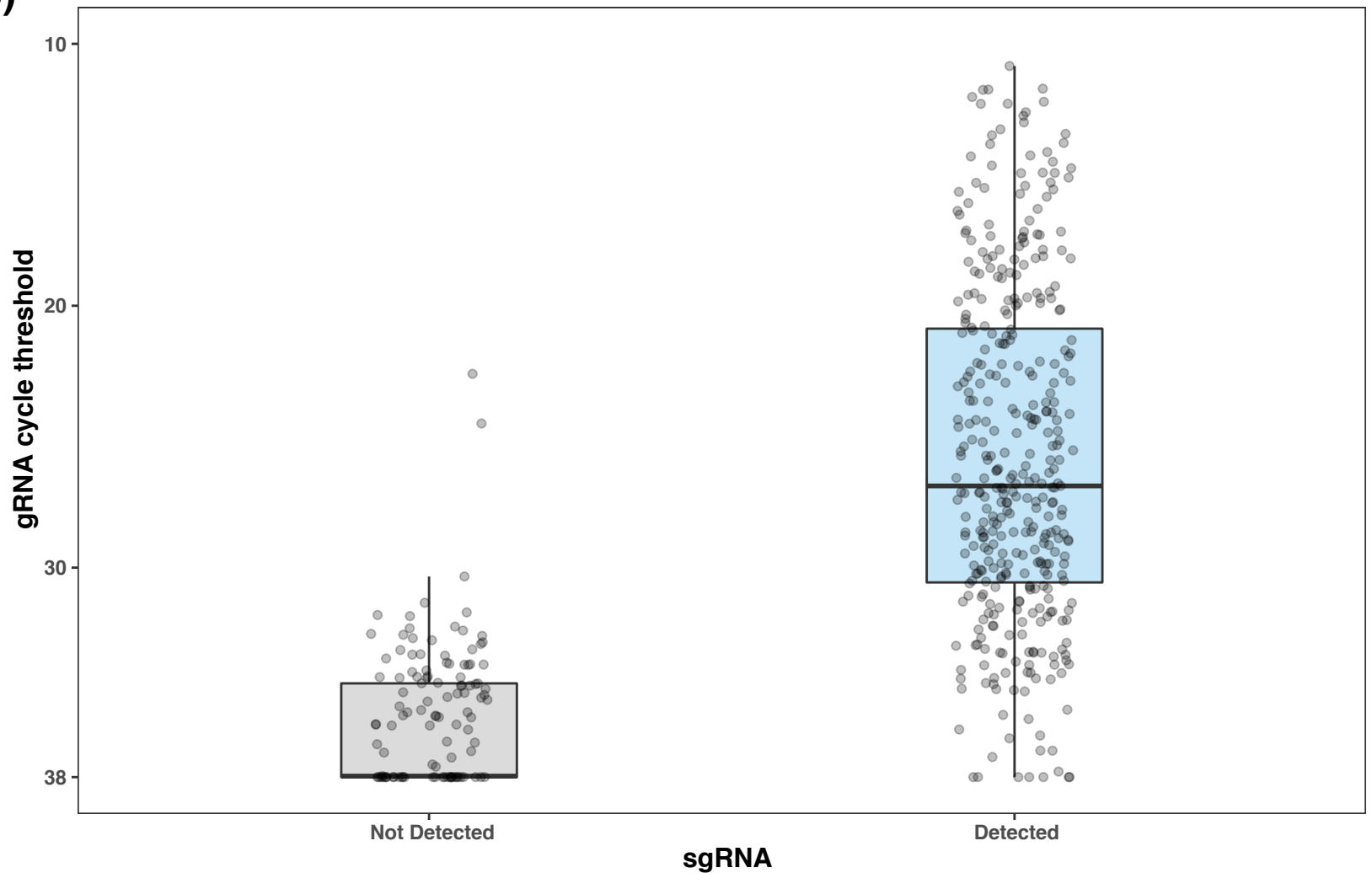
518

519

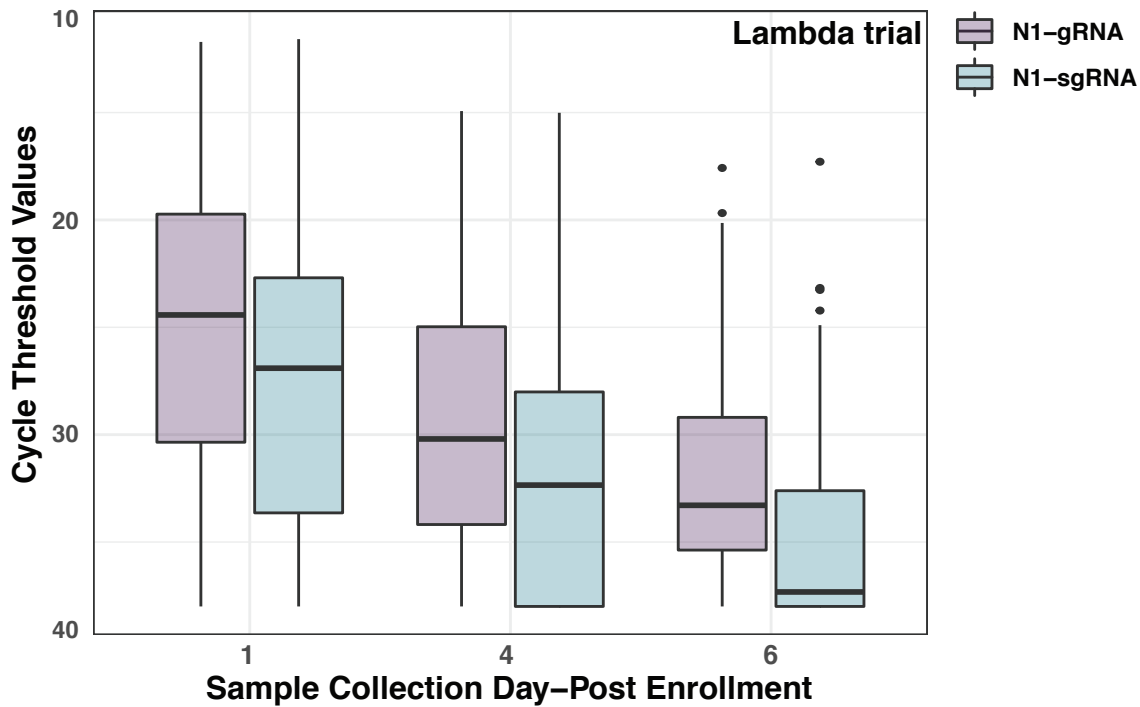
520

521

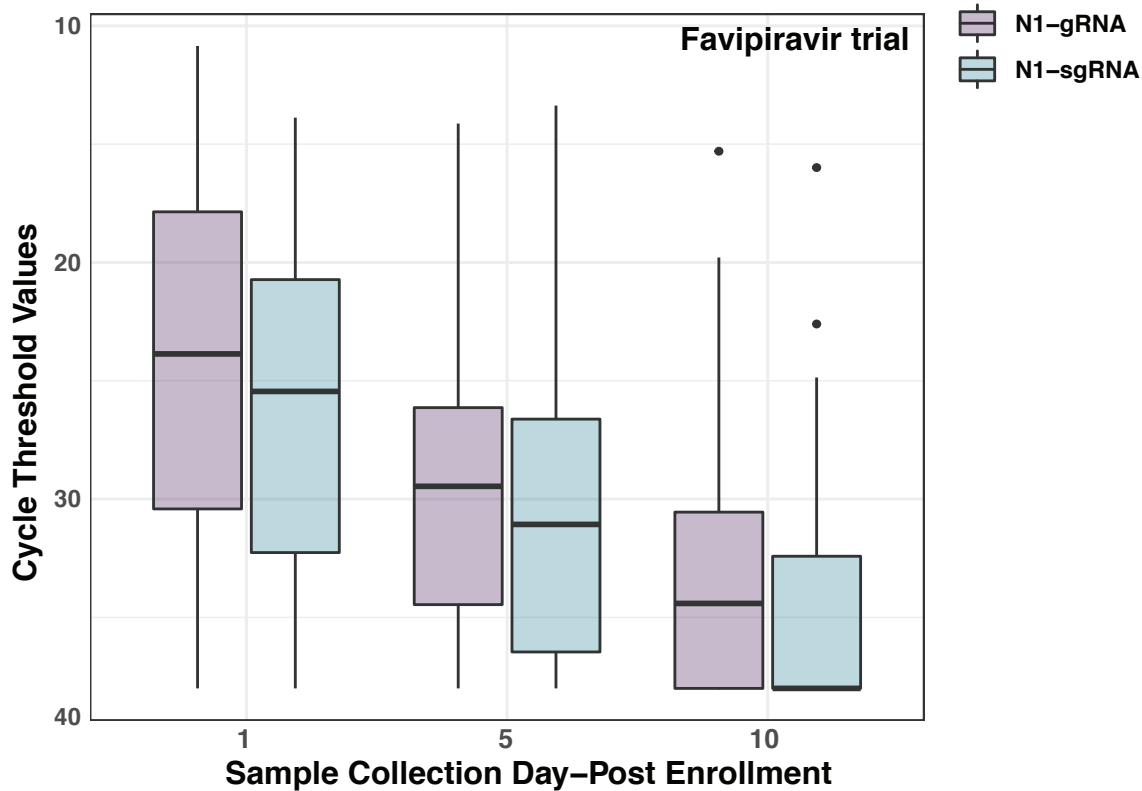
522 **Supplementary Table 1:** RT-qPCR data on N-gene genomic and sgRNA degradation analysis in  
523 remdesivir and DMSO-treated A549<sup>ACE2+</sup> cells. The cells were infected with SARS-CoV-2 at 24,  
524 48hpi, 72hpi and 96hpi. Total number of copies per samples corresponding to Ct values were  
525 calculated from standard curves using a standard curve derived from pET21b+ plasmids with the  
526 target insert.  
527  
528

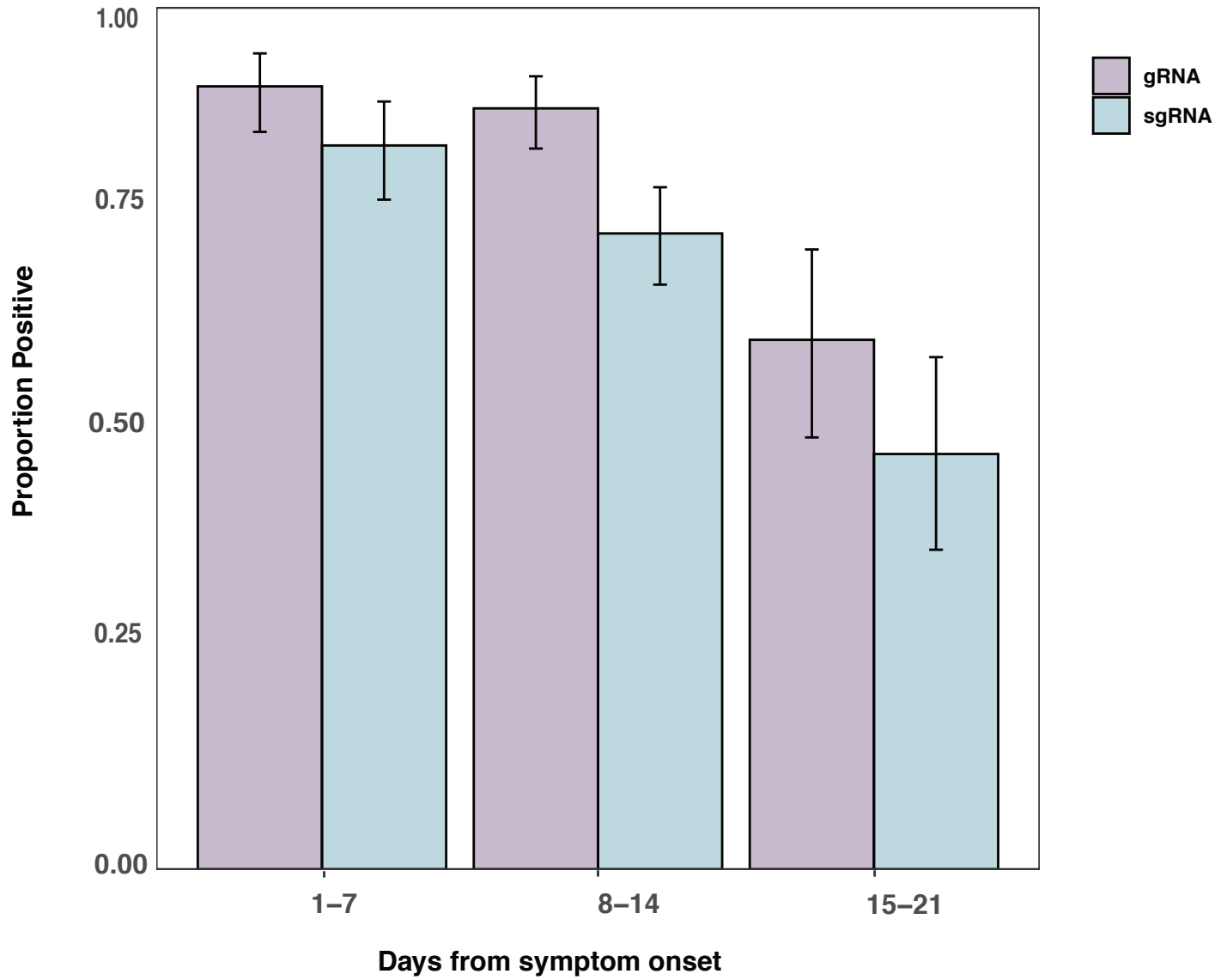
**(A)****(B)**

(A)

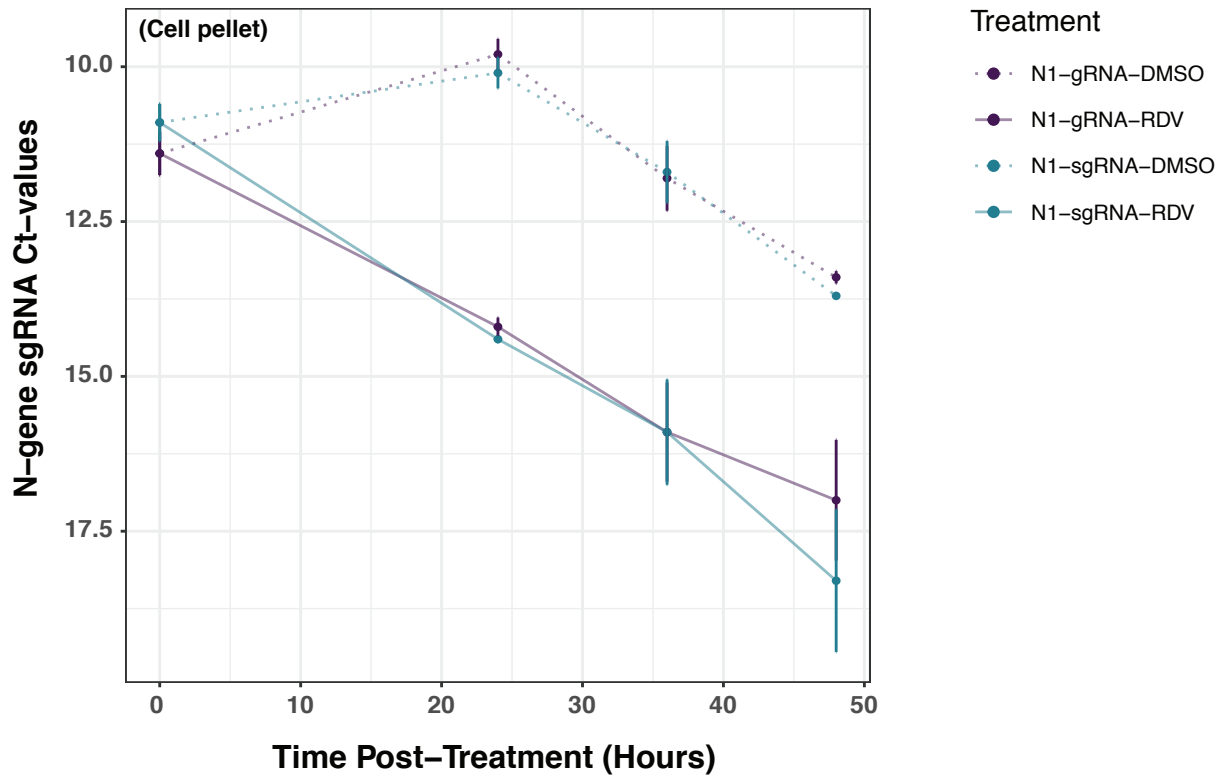


(B)

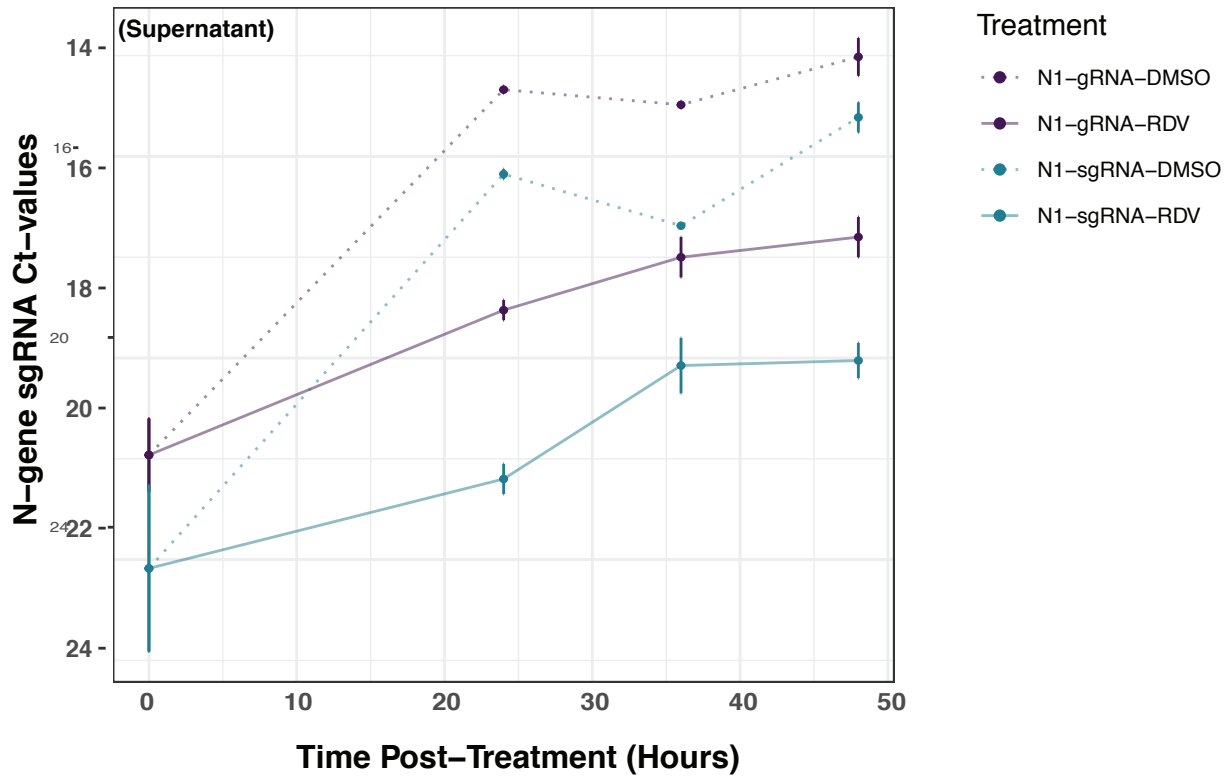




(A)

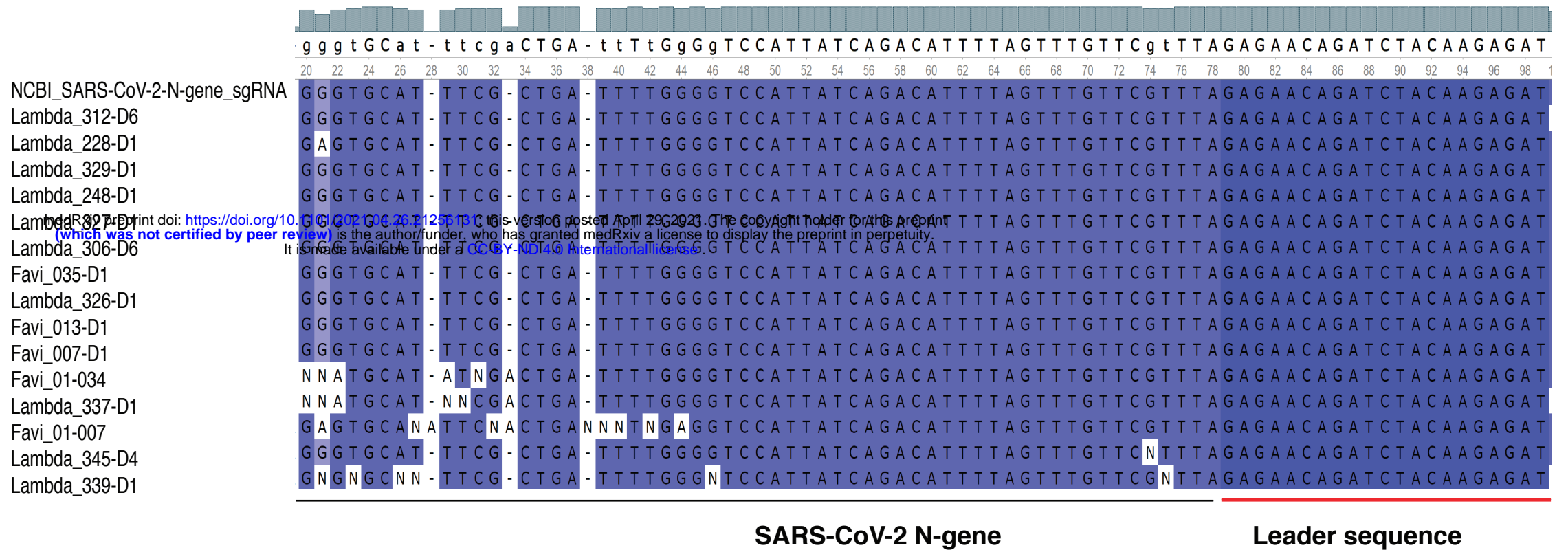


(B)

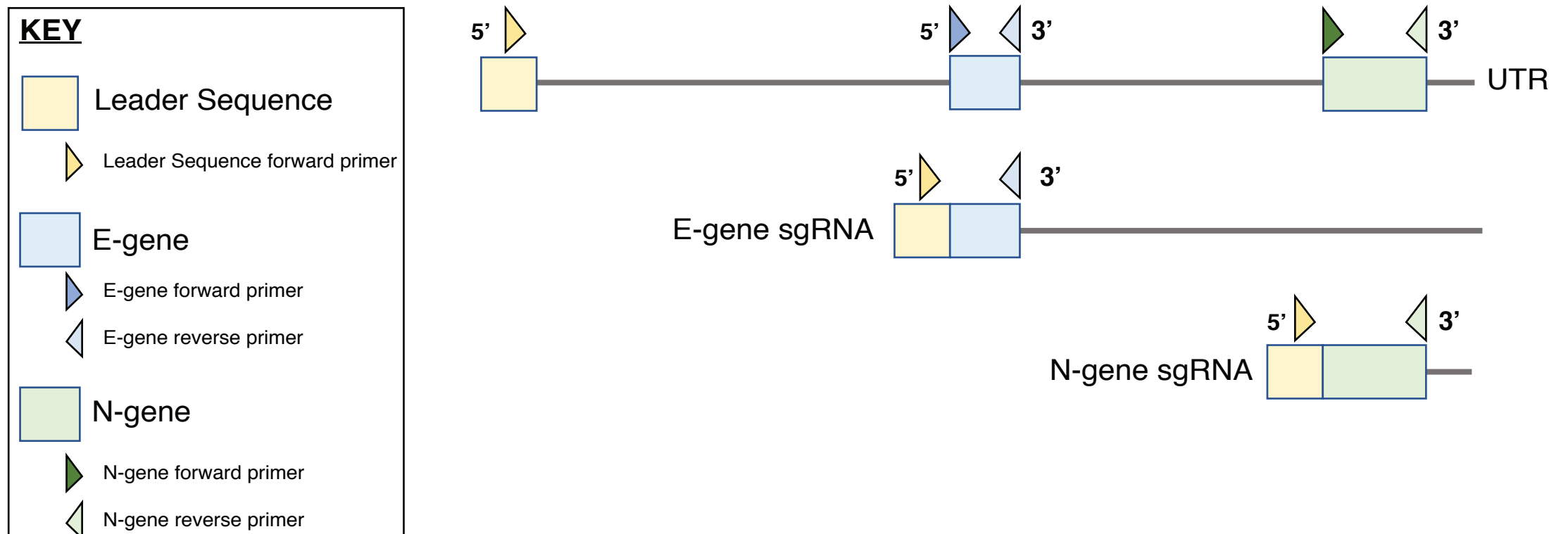


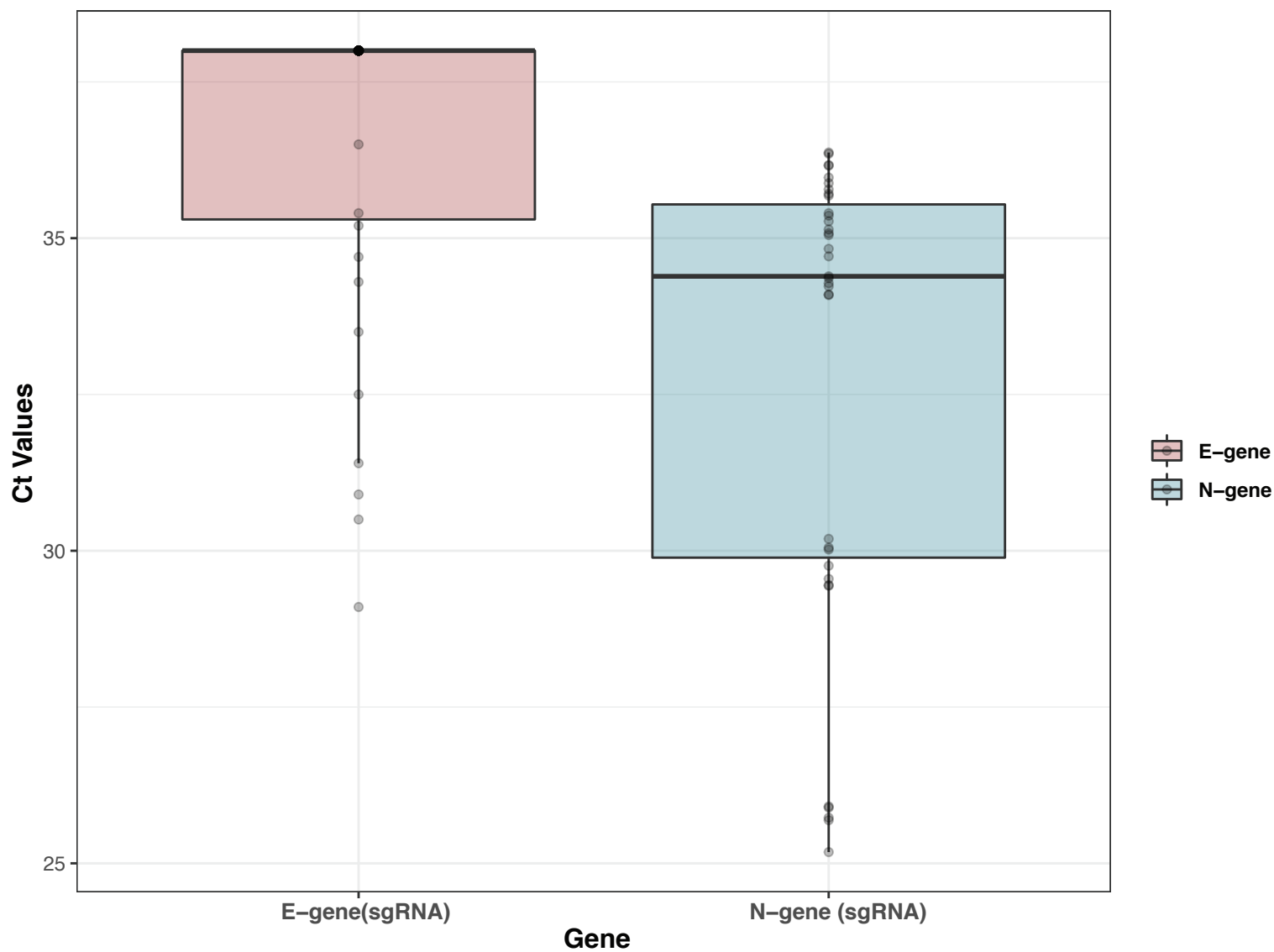


(A)

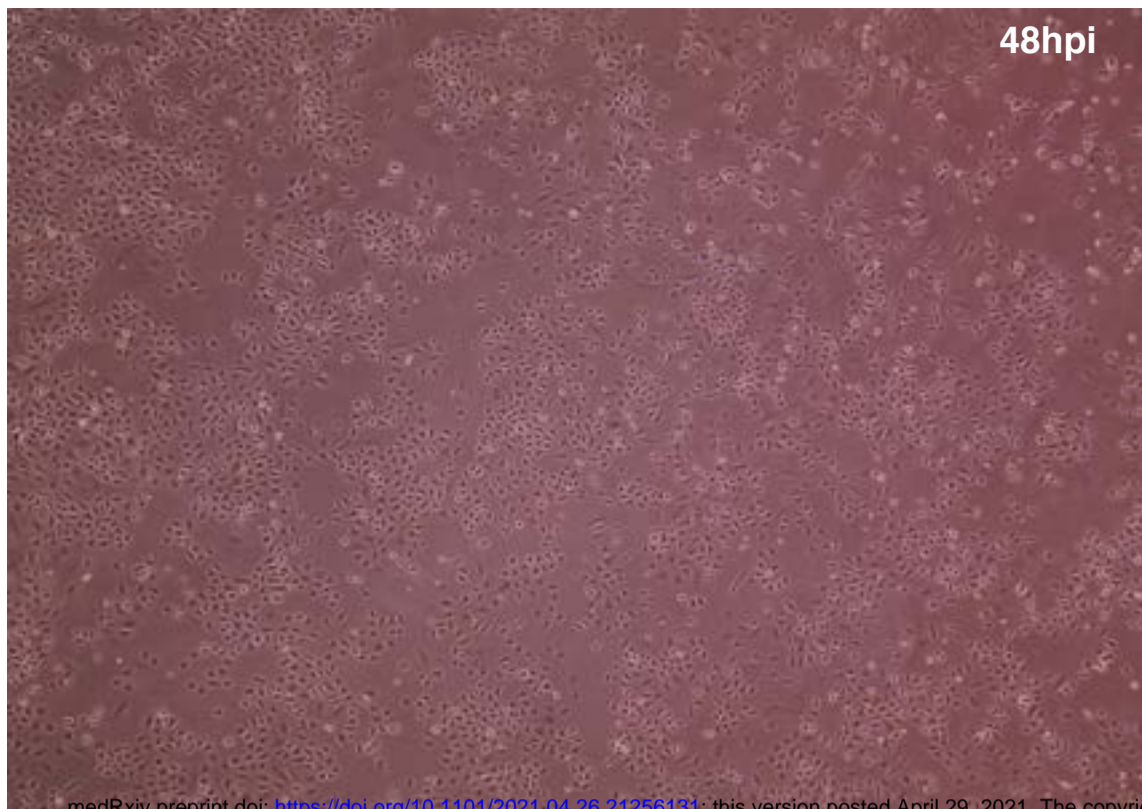


(B)





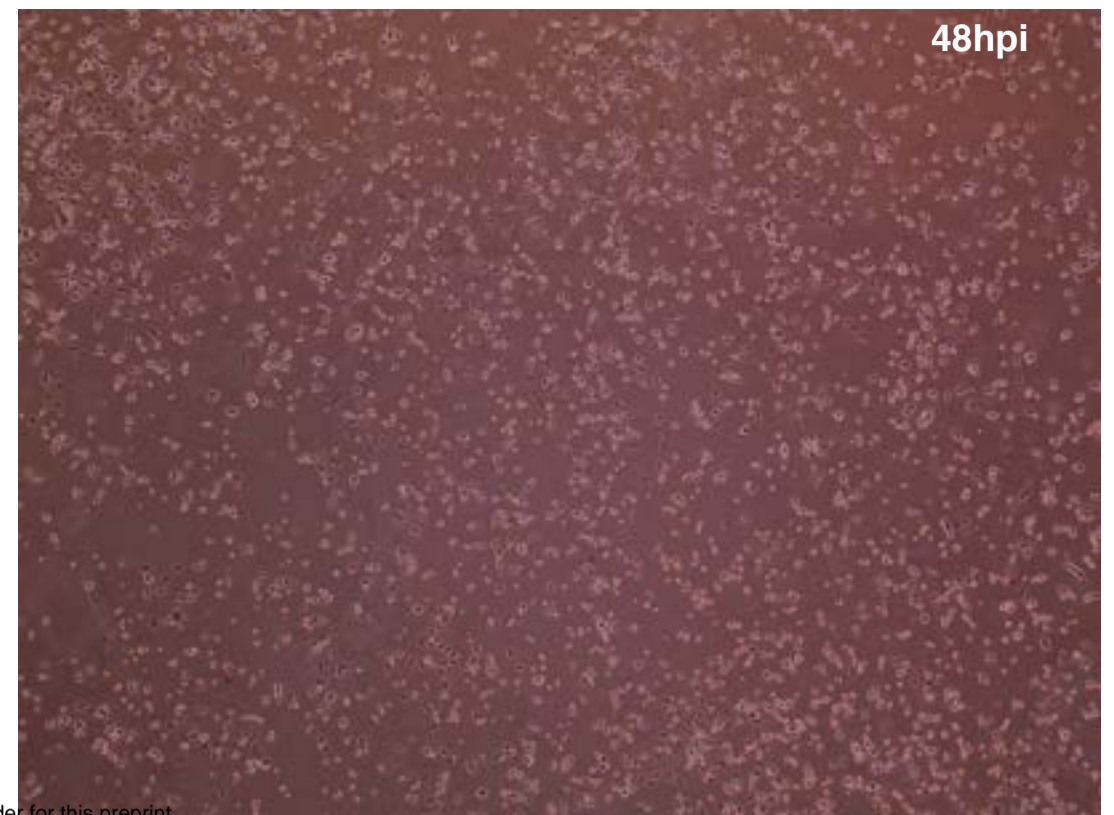
(A)



medRxiv preprint doi: <https://doi.org/10.1101/2021.04.26.21256131>; this version posted April 29, 2021. The copyright holder for this preprint (which was not certified by peer review) is the author/funder, who has granted medRxiv a license to display the preprint in perpetuity. It is made available under a [CC-BY-ND 4.0 International license](https://creativecommons.org/licenses/by-nd/4.0/).

**10uM Remdesivir treated- A549ACE2+ cells infected with SARS-CoV-2**

(B)



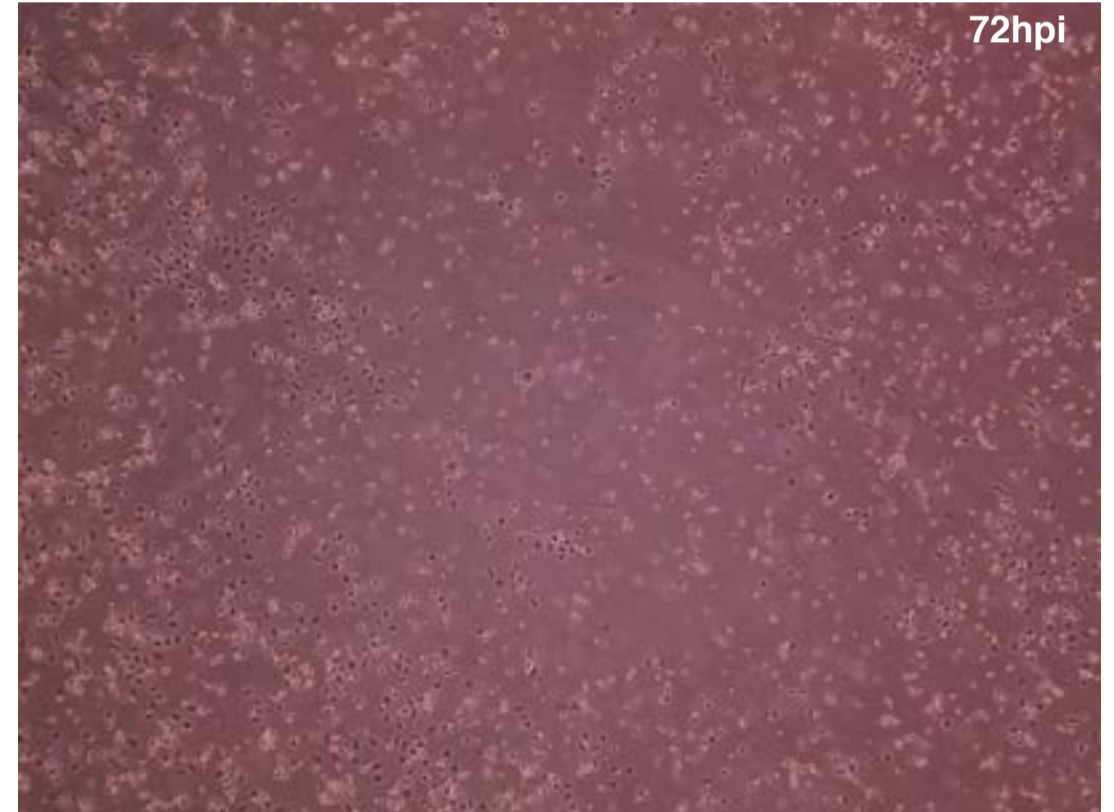
**0.1% DMSO treated- A549ACE2+ cells infected with SARS-CoV-2**

(C)



**10uM Remdesivir treated- A549ACE2+ cells infected with SARS-CoV-2**

(D)



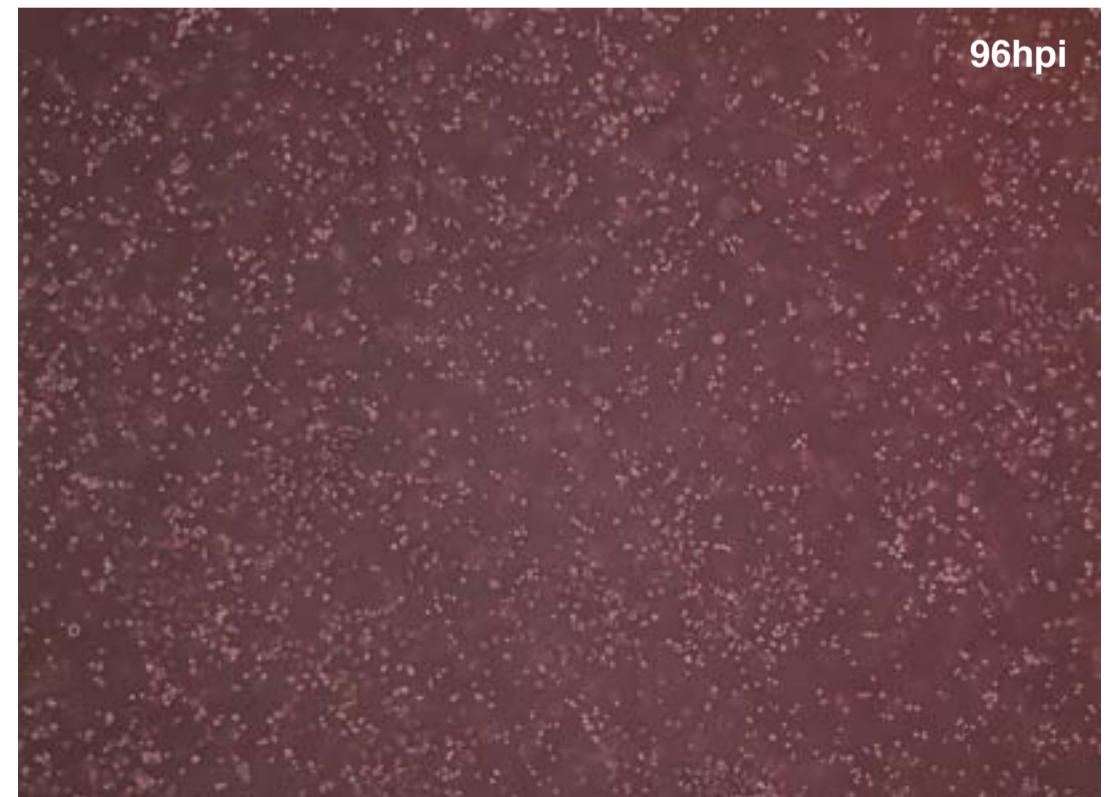
**0.1% DMSO treated- A549ACE2+ cells infected with SARS-CoV-2**

(E)



**10uM Remdesivir treated- A549ACE2+ cells infected with SARS-CoV-2**

(F)



**0.1% DMSO treated- A549ACE2+ cells infected with SARS-CoV-2**